Available online at www.sciencedirect.com
SCIENCE DIRECT®
Surface Science 572 (2004) 261–268
SURFACE SCIENCE
www.elsevier.com/locate/susc

Adsorption and reaction of 1,3-butadiene on Pt(1 1 1) and Sn/Pt(1 1 1) surface alloys

Haibo Zhao, Bruce E. Koel *

Department of Chemistry, University of Southern California, Los Angeles, CA 90089-0482, USA

Received 23 July 2004; accepted for publication 31 August 2004
Available online 15 September 2004

Abstract

Temperature-programmed desorption (TPD), Auger electron spectroscopy (AES), and low-energy electron diffraction (LEED) were used to study the chemistry of 1,3-butadiene ($H_2C{=}CHCH{=}CH_2$, C_4H_6) on Pt(1 1 1) and p(2 × 2)-Sn/Pt(1 1 1) and ($\sqrt{3} \times \sqrt{3}$)R30°-Sn/Pt(1 1 1) surface alloys. All chemisorbed 1,3-butadiene completely dehydrogenated to H_2 and surface carbon on Pt(1 1 1). Alloying Sn on Pt(1 1 1) can completely inhibit this decomposition and 1,3-butadiene reversibly adsorbs and desorbs from the two Sn/Pt(1 1 1) alloys under UHV conditions. The desorption activation energy of 1,3-butadiene on the (2 × 2) and ($\sqrt{3} \times \sqrt{3}$)R30°-Sn/Pt(1 1 1) surface alloys is 88 and 75 kJ/mol, respectively. These values are good estimates of the adsorption energies, and also place lower limits on the activation energy barrier for dissociating vinylic C–H bonds on the (2 × 2) and $\sqrt{3}$ surface alloys. Even though 1,3-butadiene is much more strongly chemisorbed than 1-butene ($H_2C{=}CHCH_2CH_3$, C_4H_8) on the (2 × 2)-Sn/Pt(1 1 1) alloy, 1,3-butadiene *is less reactive* than 1-butene because there are no allylic β-CH bonds in 1,3-butadiene as there are in 1-butene.

Keywords: Alkenes; Chemisorption; Platinum; Tin; Alloys; Thermal desorption; Auger electron spectroscopy; Low energy electron diffraction (LEED)

1. Introduction

Chemisorption of alkenes on Pt(1 1 1) has been investigated rather extensively because of the fundamental interest in the chemistry of these molecules as reactants, products and intermediates in hydrocarbon conversion over Pt-based catalysts [1–5]. Surface science studies of the chemistry of acetylene ($HC{\equiv}CH$, C_2H_2) [6–13] and 1,3-butadiene ($H_2C{=}CHCH{=}CH_2$, C_4H_6) [4,14,15] on Pt(1 1 1) have also been carried out in part due to the industrial importance of partial hydrogenation of dienes and alkynes [16,17]. The activity and selectivity for such reactions strongly depend on the metal used as a catalyst. Two metallic systems, Pd and Pt, have been the focus of most

* Corresponding author. Tel.: +1 213 740 4126; fax: +1 213 740 3972.
E-mail address: koel@usc.edu (B.E. Koel).

0039-6028/$ - see front matter © 2004 Elsevier B.V. All rights reserved.
doi:10.1016/j.susc.2004.08.039

fundamental studies of the hydrogenation of hydrocarbons [18]. For example, butadiene is preferentially hydrogenated to form butane ($H_3CCH_2CH_2CH_3$, C_4H_{10}) over Pt [19].

Generally, the addition of Sn to supported Pt catalysts for hydrocarbon conversion decreases the catalytic activity, but increases the selectivity for unsaturated hydrocarbon products and reduces coking, a poisoning of the catalyst that decreases its useful lifetime due to carbon accumulation from non-specific dehydrogenation. Bimetallic Pt–Sn catalysts are particularly promising for a variety of selective dehydrogenation and hydrogenation reactions. For example, Cortright and coworkers [20–22] have reported a highly active and selective Pt/Sn/K–L zeolite catalyst for isobutene dehydrogenation in which Pt–Sn alloy particles are clearly formed. The reduced reactivity of Pt–Sn alloy surfaces provides a simple explanation for why bimetallic Pt–Sn catalysts may have an increased selectivity for producing alkenes from the hydrogenation of dienes over that of Pt catalysts. Fundamental understanding of adsorption and reaction of 1,3-butadiene on well-defined Pt–Sn alloys would provide important information for understanding and improving Pt–Sn catalysts for use in diene hydrogenation.

Adsorption of 1,3-butadiene on Pt(1 1 1) has been studied experimentally by temperature programmed desorption (TPD) [4], high-resolution electron energy loss spectroscopy (HREELS) [4,14,15], and near-edge X-ray absorption fine structure (NEXAFS) [14,15]. Avery and Sheppard [4] concluded that chemisorption occurred via di-σ-bonding of both C=C bonds in the molecule in a tetra-σ-bonding configuration without any overall hydrogen loss at 300 K. This picture is supported by recent DFT calculations [23,24]. However, Bertolini and coworkers [14,15] argued that only the carbon atoms at the ends of the molecule form σ bonds to the Pt(1 1 1) surface, in a 1,4-di-σ-bonding configuration, and chemisorption is accompanied by the formation of a new C=C bond at the center of the molecule. This is consistent with an older calculation by Baetzold [25].

Alloying Sn in a Pt(1 1 1) surface greatly changes the reactivity of the surface and weakens the interaction with adsorbed molecules [26–28]. Under UHV conditions, decomposition of alkenes is totally inhibited on the $(\sqrt{3}\times\sqrt{3})$R30°-Sn/Pt(1 1 1) alloy and greatly decreased on the (2×2)-Sn/Pt(1 1 1) alloy [26–28]. 1,3-butadiene contains two C=C double bonds, and thus is expected to have a much stronger interaction with these alloys (barring severe steric constraints due to Sn). Stronger adsorption often leads to higher reactivity and so this is a interesting molecule to probe C–H bond cleavage barriers on these alloy surfaces.

In this paper, we investigated adsorption, desorption, and dehydrogenation of 1,3-butadiene on Pt(1 1 1), the (2×2)-Sn/Pt(1 1 1) and $(\sqrt{3}\times\sqrt{3})$R30°-Sn/Pt(1 1 1) surface alloys. We examined the influence of alloy structure on the chemistry of 1,3-butadiene and compared the reactivity of this molecule, as a prototype diene, with that of the alkenes, ethylene ($H_2C=CH_2$, C_2H_4) and 1-butene ($H_2C=CHCH_2CH_3$, C_4H_8).

2. Experimental methods

Experiments were performed in a three-level UHV chamber as described earlier [29]. The Pt(1 1 1) crystal (Atomergic; 10-mm dia., 1.5-mm thick) was prepared by using 1-keV Ar^+-ion sputtering and oxygen exposures (5×10^{-7}-Torr O_2, at 900 K for 2 min) to give a clean spectrum in Auger electron spectroscopy (AES) and a sharp (1×1) pattern in low energy electron diffraction (LEED).

The (2×2)Sn/Pt(1 1 1) and $(\sqrt{3}\times\sqrt{3})$R30°Sn/Pt(1 1 1) surface alloys were prepared by evaporating one monolayer of Sn onto the Pt(1 1 1) crystal surface and subsequently annealing the sample for 20 s to 1000 K and 830 K, respectively. Sn is incorporated substitutionally into primarily only the surface layer to form an ordered alloy or intermetallic compound with $\theta_{Sn} = 0.25$, with a composition corresponding to the (1 1 1) face of a bulk Pt_3Sn crystal, and $\theta_{Sn} = 0.33$, with a composition corresponding to a Pt_2Sn surface. These surface alloys are relatively "flat", but Sn atoms protrude 0.02 nm above the surface-Pt plane at both surfaces [30]. In the (2×2) structure, pure-Pt three-fold reactive sites are present, but no adjacent pure-Pt three-fold sites exist. All pure-Pt three-fold

sites are eliminated in the $(\sqrt{3}\times\sqrt{3})R30°$ structure, and only two-fold pure Pt sites are present. For brevity throughout this paper, we will refer to the p(2 × 2)-Sn/Pt(1 1 1) and $(\sqrt{3}\times\sqrt{3})R30°$-Sn/Pt(1 1 1) surface alloys as the (2 × 2) and $\sqrt{3}$ alloys, respectively.

1,3-Butadiene (C_4H_6, Matheson, 99.5%) was used without additional purification. The gas was exposed on the Pt crystal by a microcapillary array doser connected to a gas line through a variable leak valve. All of the exposures reported here are given simply in terms of the background pressure in the UHV chamber as measured by an ion gauge. No attempt was made to correct for the flux enhancement of the doser or ion gage sensitivity. The mass spectrometer in the chamber was used to check the purity of the gases during dosing.

For all TPD experiments, the heating rate was 3.6 K/s and all exposures were given with the surface temperature at 100 K. AES measurements were made with a double-pass cylindrical mirror analyzer (CMA) using a modulation voltage of 4 eV. The electron gun was operated at 3-keV beam energy and 1.5-μA beam current. Coverages θ_i reported in this paper are referenced to the surface atom density of Pt(1 1 1) such that θ_{Pt} = 1.0 ML is defined as $1.505\times10^{15}\,cm^{-2}$.

3. Results

Fig. 1 shows butadiene, C_4H_6, TPD spectra after different 1,3-butadiene exposures on Pt(1 1 1) at 100 K. At low exposures, no molecular C_4H_6 desorbs upon heating. Increasing butadiene exposures leads to desorption from the physisorbed layer at 130 K. At any coverage, the chemisorbed layer of butadiene decomposes and only H_2 is detected in the TPD spectra. The dehydrogenation of butadiene leads to the build up of surface carbon on Pt(1 1 1), which is detected by AES following TPD experiments. Our results agree with the TPD results of Avery and Sheppard [4].

H_2 evolution, as shown in Fig. 2, monitors complete butadiene decomposition on Pt(1 1 1). The amount of H_2 desorption saturates at 0.18-L exposure, where the butadiene monolayer saturation coverage was reached as determined by monitoring C_4H_6 desorption in Fig. 1. Three H_2 desorption peaks can be identified at 370, 398 and 585 K, which indicates that several steps are needed to complete the decomposition process. At low coverage, the first H_2 desorption peak appears at 339 K and no peak at 398 K is detected. This shift indicates that co-adsorbed hydrocarbon fragments produced from dehydrogenation increases the C–H bond cleavage barrier. The total, amount of H_2 evolved in TPD after large exposures of butadiene is 0.44 ML H_2, corresponding to the complete decomposition of 0.15-ML C_4H_6. This value was determined by comparison of this H_2 TPD peak area to a reference H_2 TPD spectrum obtained after ethylene (C_2H_4) exposures on Pt(1 1 1) at 300 K to produce 0.25-ML ethylidyne (CCH_3) [31], in which complete decomposition produces 0.375-ML H_2, i.e. 0.75 ML H. Since complete dehydrogenation is the only reaction pathway for chemisorbed C_4H_6, the saturation coverage of C_4H_6 on Pt(1 1 1) is 0.15 ML.

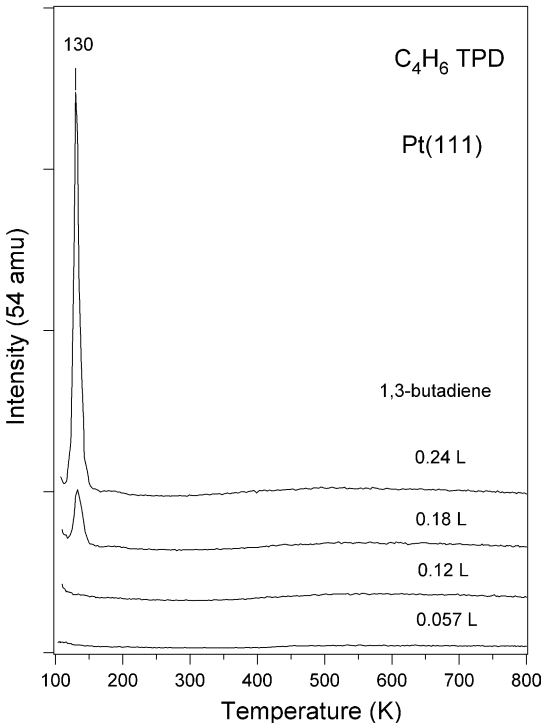

Fig. 1. Butadiene (C_4H_6) TPD spectra after 1,3-butadiene exposures on Pt(1 1 1) at 100 K.

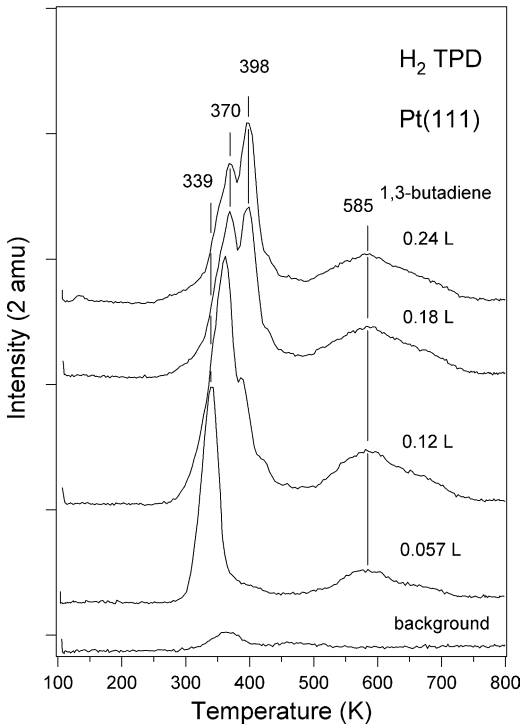

Fig. 2. H_2 TPD spectra after 1,3-butadiene exposures on Pt(1 1 1) at 100 K.

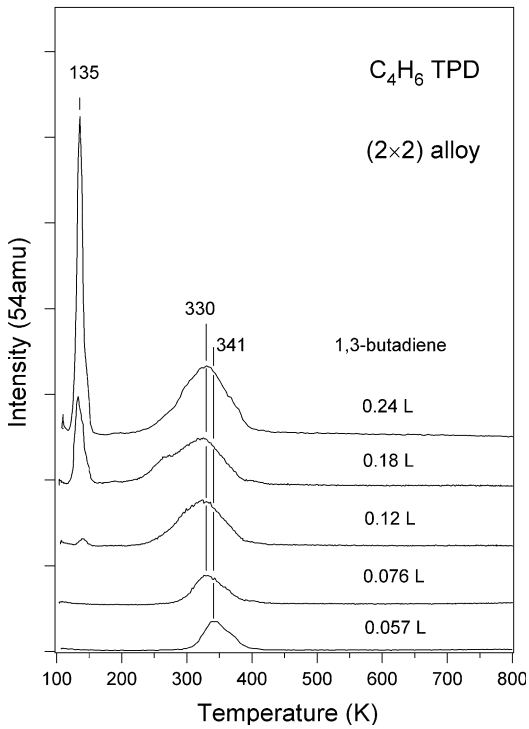

Fig. 3. Butadiene (C_4H_6) TPD spectra after 1,3-butadiene exposures on the (2 × 2)-Sn/Pt(1 1 1) alloy at 100 K.

In Fig. 3, a series TPD spectra are shown for C_4H_6 following 1,3-butadiene dosing on the (2 × 2) surface alloy at 100 K. Butadiene from the chemisorbed layer desorbs at 341 K at low coverage and this shifts to 330 K at monolayer coverage. Desorption from the physisorbed layer is observed at 135 K at high coverage. Assuming first-order desorption kinetics with a preexponential factor of $10^{13}\,s^{-1}$, the Redhead method [32] was used to estimate a desorption activation energy E_d of 88 kJ/mol for C_4H_6 adsorbed on the (2 × 2) alloy at low coverage.

In Fig. 4, a series of C_4H_6 TPD spectra are shown following 1,3-butadiene dosing on the $\sqrt{3}$ alloy at 100 K. Butadiene from the chemisorbed layer desorbed at 292 K at low coverage and this shifted to 275 K at monolayer coverage. Desorption from a physisorbed layer was observed at 121 and 145 K at high coverages. A value for E_d of 75 kJ/mol on the $\sqrt{3}$ alloy was obtained by Redhead analysis using the peak at low coverage. We note that the desorption peak width of chemisorbed butadiene on the $\sqrt{3}$ alloy is appreciably narrower than that on the (2 × 2) alloy. This might mean that butadiene chemisorbs on the (2 × 2) alloy in more than one bonding configuration.

H_2 evolution shown in Fig. 5 monitors butadiene decomposition on Pt(1 1 1) and the (2 × 2) and $\sqrt{3}$ alloys at monolayer coverage. In contrast to the complete dehydrogenation of butadiene on Pt(1 1 1), no significant H_2 desorption was observed (or at any butadiene coverage used in these experiments) on the two Sn/Pt(1 1 1) surface alloys. The small H_2 desorption features are mostly due to cracking fractions from butadiene desorption and the residual yield is almost at the same level as that in "background" TPD experiments where no exposure to butadiene was given. This is consistent with AES that detected no carbon on the two alloys after any TPD experiment. Therefore, butadiene thermal decomposition was completely suppressed under these conditions upon forming

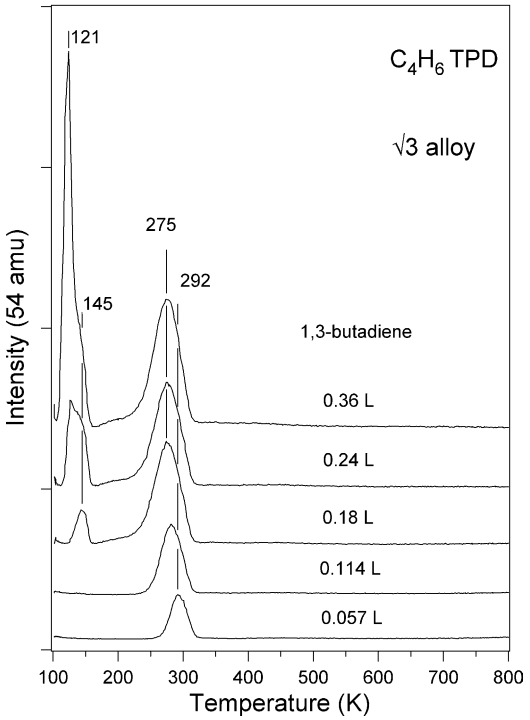

Fig. 4. Butadiene (C_4H_6) TPD spectra after 1,3-butadiene exposures on the ($\sqrt{3}\times\sqrt{3}$)R30°-Sn/Pt(1 1 1) alloy at 100 K.

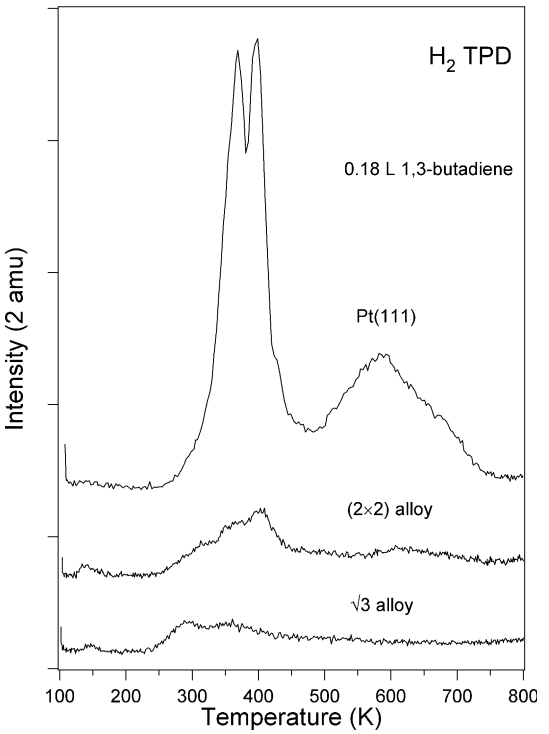

Fig. 5. Comparison of H_2 desorption spectra resulting from 1,3-butadiene decomposition on Pt(1 1 1) and the (2 × 2)-Sn/Pt(1 1 1) and ($\sqrt{3}\times\sqrt{3}$)R30°-Sn/Pt(1 1 1) alloys.

the two alloys. 1,3-Butadiene reversibly adsorbs and desorbs on these two Sn/Pt(1 1 1) surface alloys.

Using the relationship between C_4H_6 TPD peak area and butadiene coverage deduced from the data in Figs. 1 and 2, as described in Appendix A, we can calculate the unknown butadiene monolayer coverage on each alloy by using the C_4H_6 TPD peak area in spectra from the chemisorbed monolayer on the two alloys. This approach gives values of 0.15 and 0.17 ML on the (2 × 2) and $\sqrt{3}$ alloy, respectively.

4. Discussion

At 300 K, 1,3-butadiene is believed to chemisorb on Pt(1 1 1) in a tetra-σ-bonding configuration [4,23,24], without any dehydrogenation of the molecule [4]. Fig. 2 shows that no H_2 evolution occurs before 300 K, which is an experimental result consistent with that reported by Avery and Sheppard [4]. An older theoretical study by Baetzold [25] predicted that 1,3-butadiene would decompose via loss of two terminal hydrogens to form a $(CH)_4$ metallacycle, but the data in Fig. 2 shows that this decomposition mechanism is not correct. At low exposure (0.057-ML C_4H_6), the H_2 desorption peak area ratio at 339 K to 585 K is larger than 4:2, rather than the 2:4 ratio predicted by the theory.

The presence of Sn in the surface layer of Pt(1 1 1) greatly weakened the interaction between 1,3-butadiene and the alloy surface. Increasing the Sn concentration from 25% to 33% leads to a decrease in the desorption activation energy E_d from 88 to 75 kJ/mol. This is also a good estimate of the adsorption energy in this case where there is no appreciable activation energy barrier to adsorption. This effect of Sn on the adsorption energy has been observed for alkenes [26–28] and many other molecules as well. The adsorption energy of

1,3-butadiene on the (2×2) and $\sqrt{3}$ alloys is roughly 1.5 times that of ethylene [26] and 1-butene [27] on the same alloy. Ethylene chemisorbs on Pt(1 1 1) and the two Sn/Pt(1 1 1) alloys via di-σ-bonding, but the carbon atoms in chemisorbed ethylene are less rehybridized toward sp^3 with increasing Sn in the surface layer [26]. A comparison of adsorption energies between 1,3-butadiene and 1-butene or ethylene suggests that all four carbon atoms in 1,3-butadiene should have strong interactions with the alloy surfaces. We propose that 1,3-butadiene chemisorbs on the two Sn/Pt(1 1 1) alloys in a tetra-σ-bonding configuration, as on Pt(1 1 1), but with the carbon atoms less sp^3-rehybridized than that on Pt(1 1 1). The presence of Sn in the surface layer of Pt(1 1 1) has no effect, however, on the chemisorbed monolayer coverage of 1,3-butadiene. This coverage is identical on Pt(1 1 1) and the (2×2) alloy, and even slightly higher on the $\sqrt{3}$ alloy. Such behavior has also been observed in studies of other alkene and alkane molecules [27,28,33]. This is probably due to a small relaxation in the bonding geometry/site requirements that result from slightly weaker bonding interactions between the chemisorbed molecule and the $\sqrt{3}$ alloy surface.

All of the butene isomers, along with propene, undergo an appreciable amount of decomposition (7–10%) on the (2×2) alloy. Even though the adsorption energy of 1,3-butadiene is 1.5 times that of 1-butene or 2-butene [27], the decomposition of 1,3-butadiene is completely inhibited on the (2×2) alloy, like that observed for ethylene [26]. This result, which is surprising at first glance, can be explained simply by the presence of relatively weak allylic β-CH bonds in propene and butene. Only vinylic CH bonds exist in ethylene and 1,3-butadiene, and these bonds have a higher bond dissociation energy than allylic β-CH bonds [34]. So, these vinylic CH bonds are appreciably less reactive on Pt(1 1 1) and these alloys. The 1,4-di-σ-bonded configuration of 1,3-butadiene on Pt(1 1 1) proposed by Bertolini and coworkers [14,15] may not be appropriate, particularly on the (2×2) alloy, because this configuration would create allylic β-CH bonds on the end carbon atoms and this would pretty clearly lead to decomposition on the surface.

Like all of the small alkene molecules, 1,3-butadiene reversibly adsorbs and desorbs on the $\sqrt{3}$ alloy. The origin of this decreased reactivity compared to that on Pt(1 1 1) was explained originally for ethylene as an increase in the activation energy for C–H bond scission, E^* on the alloys. However, this was never quite clear because the ethylene adsorption energy also decreased on these two Sn/Pt(1 1 1) alloys, and this could also lead to increased desorption and lack of reaction under UHV conditions. Now, because of the much larger desorption activation energy for 1,3-butadiene compared to ethylene on these two Sn/Pt(1 1 1) alloys, we can exclude this latter rationale which uses the decrease in desorption activation energy by alloying Sn to Pt(1 1 1). We now show that ethylene decomposition is inhibited because of the increase in E^* the C–H bond breaking barrier, on the alloys. Also, now we can place a much better lower limit for E^* of vinylic CH bonds of 88 and 75 kJ/mol on the (2×2) and $\sqrt{3}$ alloys, respectively. The increase in this barrier may be caused by site-blocking or by electronic modifications of the Pt(1 1 1) surface by alloying with Sn. In the (2×2) structure, pure-Pt three-fold reactive sites are present, but no adjacent pure-Pt three-fold sites exist. All pure-Pt three-fold sites are eliminated in the $(\sqrt{3}\times\sqrt{3})R30^\circ$ structure, and only two-fold pure Pt sites are present. Alloying also changes the local electronic structure at Pt sites. Calculations by Pick [35] and Delbecq and Sautet [36] consider that a shift of the Pt d-band center resulting from charge transfer from Sn to Pt decreases the bond strength between adsorbed molecules and Sn–Pt alloys. Such changes could also leads to the formation of a significant activation energy barriers for bond dissociation reactions of adsorbed molecules.

5. Conclusions

On Pt(1 1 1), chemisorbed 1,3-butadiene completely decomposed to H_2 and surface carbon upon heating. This decomposition pathway is completely inhibited on two Sn/Pt(1 1 1) surface alloys. Alloyed Sn also reduces the chemisorption bond strength of 1,3-butadiene compared to that

on Pt(1 1 1). The desorption activation energy E_d for 1,3-butadiene on the (2×2) and $(\sqrt{3}\times\sqrt{3})$-R30°-Sn/Pt(1 1 1) alloys is 88 and 75 kJ/mol, respectively. However, alloyed Sn has no effect on the coverage of 1,3-butadiene in the chemisorbed monolayer, which is 0.15, 0.15, and 0.17 ML on Pt(1 1 1) and the (2×2) and $(\sqrt{3}\times\sqrt{3})$R30°-Sn/Pt(1 1 1) surface alloys, respectively. We propose that the lack of reactivity of ethylene and 1,3-butadiene on these alloys is due to lack of allylic β-CH bonds. Because E_d for 1,3-butadiene on these alloys is 1.5 times that of ethylene or 1-butene on the same surface, we can now set a more useful lower limit for the vinylic C–H bond breaking barrier E^* on these alloys of 88 kJ/mol.

Acknowledgment

This work was supported by the Department of Energy, Office of Basic Energy Sciences, Chemical Sciences Division.

Appendix A

Herein we derive the relationship between butadiene TPD peak area and butadiene coverage by using data from Fig. 1 in order to calculate the monolayer coverage of butadiene on the alloys from the areas of the TPD peaks obtained from the two alloy surfaces.

Surface coverage θ is related to gas exposure ε by $\theta = S\varepsilon$ where S is the sticking coefficient. Assuming that the butadiene sticking coefficient is a constant value over the monolayer and multilayer regime on Pt(1 1 1) at 100 K, as has been shown for similar molecules many times before, then there is a simple relationship $\theta_2/\theta_1 = \varepsilon_2/\varepsilon_1$ between two different coverages produced by two different exposures. TPD peak areas are also related to surface coverages by a factor X that is unknown but is a constant and has units of ML^{-1}. This factor for butadiene can be determined from the butadiene TPD curves from Pt(1 1 1) shown in Fig. 1, along with information that the monolayer coverage of butadiene θ_{mono} is 0.15 ML, as derived from the H_2 TPD data of Fig. 2. Butadiene exposures of 0.18 and 0.24 L produce a butadiene coverage on the surface that exceeds one monolayer, and the total amount is given by $\theta_{multi} + \theta_{mono}$. Butadiene desorbs from the two multilayers produced by these two exposures to yield desorption peak areas of 7842 and 53 912, respectively. The value of θ_{multi} is given by $7842/X$ and $53912/X$ for exposures of 0.18 and 0.24 L, respectively. Substitution into the simple relationship between coverage and exposure given above yields the following equation

$$\frac{\frac{53912}{X}+0.15}{\frac{7842}{X}+0.15}=\frac{0.24}{0.18} \quad (1)$$

that can now be solved for X. A value of $X = 869120\,ML^{-1}$ is obtained.

All of the butadiene in the monolayer desorbed molecularly on the (2×2) and $\sqrt{3}$ alloy to give butadiene desorption peak areas of 129 931 and 150 978, respectively. These peak areas are converted to monolayer coverages by dividing by X to give 0.15 and 0.17 ML on the (2×2) and $\sqrt{3}$ alloy, respectively.

References

[1] M. Salmeron, G.A. Somorjai, J. Phys. Chem. 86 (1982) 341.
[2] R.J. Koestner, J.C. Frost, P.C. Stair, M.A. Van Hove, G.A. Somorjai, Surf. Sci. 116 (1982) 85.
[3] R.J. Koestner, M.A. Van Hove, G.A. Somorjai, J. Phy. Chem. 87 (1983) 203.
[4] N.R. Avery, N. Sheppard, Proc. R. Soc. Lond. A 405 (1986) 1.
[5] K.M. Ogle, J.R. Creighton, S. Akhter, J.M. White, Surf. Sci. 169 (1986) 246.
[6] N.R. Avery, Langmuir 4 (1988) 445.
[7] W.H. Weinberg, H.A. Deans, R.P. Merill, Surf. Sci. 41 (1974) 312.
[8] L.L. Kesmodel, P.C. Stair, R.C. Baetzold, G.A. Somorjai, Phys. Rev. Lett. 36 (1976) 1316.
[9] L.L. Kesmodel, L.H. Dubois, G.A. Somorjai, J. Chem. Phys. 70 (1979) 2180.
[10] H. Ibach, S. Lehwald, J. Vac. Sci. Technol. 15 (1978) 407.
[11] P.S. Cremmer, X. Su, Y.R. Chen, G.A. Somorjai, J. Phys. Chem. B 101 (1997) 6474.
[12] P. Skinner, M. Howard, I. Oxton, S. Kettle, D. Powell, N. Sheppard, J. Chem. Soc. Faraday Trans. 15 (1978) 407.
[13] O. Nakagoe, N. Takagi, Y. Matsumoto, Surf. Sci. 514 (2002) 414.
[14] J.C. Bertolini, A. Cassuto, Y. Jugnet, J. Massardier, B. Tardy, G. Tourillon, Surf. Sci. 349 (1996) 88.

[15] G. Tourillon, A. Cassuto, Y. Jugnet, J. Massardier, J.C. Bertolini, J. Chem. Soc., Faraday Tran. 92 (1996) 92.
[16] J.P. Boitiaux, P. Cosyns, M. Derrien, G. Leger, Hydrocarbon Proc. 64 (1985) 51.
[17] M. Derrien, in: L. Cerny (Ed.), Studies in Surface Science and Catalysis, vol. 27, Elsevier, Amsterdam, 1986, p. 313.
[18] H. Arnold, F. Döbert, J. Gaube, in: G. Ertl, H. Knözinger, J. Weitkamp (Eds.), Handbook of Heterogeneous Catalysis, Wiley-VCH, Weiheim, Germany, 1997.
[19] A.J. Bates, Z.K. Leszcynski, J.J. Phillipson, P.B. Wells, G.R. Wilson, J. Chem. Soc. A (London) (1970) 2435.
[20] R.D. Cortright, J.A. Dumesic, Appl. Catal. A 129 (1995) 101.
[21] R.D. Cortright, P.E. Levin, J.A. Dumesic, Ind. Eng. Chem. Res. 37 (1998) 1717.
[22] J.M. Hill, R.D. Cortright, J.A. Dumesic, Appl. Catal. A 168 (1998) 9.
[23] F. Mittendorfer, C. Thomazeau, P. Raybaud, H. Toulhoat, J. Phy. Chem. B. 107 (2003) 12287.
[24] A. Valcárcel, A. Clotet, J.M. Ricart, F. Delbecq, P. Sautet, Surf. Sci. 549 (2004) 121.
[25] R.C. Baetzold, Langmuir 3 (1987) 189.
[26] M.T. Paffett, S.C. Gebhard, R.G. Windham, B.E. Koel, Surf. Sci. 223 (1989) 449.
[27] Y. Tsai, B.E. Koel, J. Phy. Chem. B 101 (1997) 1895.
[28] Y. Tsai, C. Xu, B.E. Koel, Surf. Sci. 385 (1997) 37.
[29] H. Zhao, J. Kim, B.E. Koel, Surf. Sci. 538 (2003) 147.
[30] S.H. Overbury, D.R. Mullins, M.T. Paffett, B.E. Koel, Surf. Sci. 254 (1991) 45.
[31] R.G. Wndham, M.E. Bartram, B.E. Koel, J. Phy. Chem. 92 (1988) 2862.
[32] P.A. Redhead, Vacuum 12 (1962) 203.
[33] C. Xu, B.E. Koel, M.T. Paffett, Langmuir 10 (1994) 166.
[34] J. Berkowitz, G. Ellison, D. Gutman, J. Phy. Chem. 98 (1994) 2774.
[35] S. Pick, Surf. Sci. 436 (1999) 220.
[36] F. Delbecq, P. Sautet, J. Catal. 220 (2003) 115.